N$_2$ Activation by Neutral Ruthenium Clusters
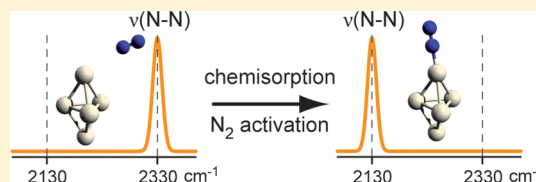
Christian Kerpal,[†] Dan J. Harding,[†] Jonathan T. Lyon,[‡] Gerard Meijer,[†] and André Fielicke*[,†,§]

[†]Fritz-Haber-Institut der Max-Planck-Gesellschaft, Faradayweg 4-6, D-14195 Berlin, Germany
[‡]Department of Natural Sciences, Clayton State University, 2000 Clayton State Boulevard, Morrow, Georgia 30260, United States
[§]Institut für Optik und Atomare Physik, Technische Universität Berlin, Hardenbergstrasse 36, D-10623 Berlin, Germany

Ⓢ *Supporting Information*

ABSTRACT: The activation of nitrogen molecules when forming complexes with neutral Ru clusters in the gas phase has been investigated by probing their N−N stretching frequencies using infrared multiple photon dissociation spectroscopy. The measured frequencies for Ru$_n$N$_{2m}$ ($n = 5$−16; $m = 1, 2$) fall in the range between 2110 and 2201 cm^{-1} and can be attributed to chemisorbed σ-bonded N$_2$, which corresponds to the γ-state on metal surfaces. The band positions are not dependent on the N$_2$ coverage, but significant variations are found depending on cluster size.

I. INTRODUCTION

Ruthenium is well-known for its remarkable catalytic abilities, including CO oxidation processes[1] and low-temperature activity in ammonia synthesis.[2,3] The latter is especially important, as ammonia synthesis via the traditional Haber−Bosch process depends on high pressures and temperatures and is therefore highly energy consuming. Pioneering work studying the catalytic properties of ruthenium has been done by Aika et al., who found that ruthenium catalyzes ammonia formation from N$_2$ and H$_2$.[4,5] Since then, promoted ruthenium has been suggested as a more efficient replacement to the traditional Haber−Bosch catalyst in ammonia synthesis, and carbon-supported ruthenium is by now industrially used as catalyst in the low-pressure ammonia synthesis of Kellogg, Brown, and Root (KBR Advanced Ammonia Process).[6]

Catalytic ammonia formation on ruthenium turns out to be a very structure-sensitive reaction.[2] One possible explanation suggests that the overall rate-determining step, shown to be the dissociation of molecular nitrogen,[7] occurs preferentially on special B5 centers, where the nitrogen molecule interacts with five ruthenium atoms.[8] Alkali metals and especially barium promote the reaction, but the mechanism is not fully clear yet.[9] Although in the past the properties of (ordered) ruthenium surfaces or supported ruthenium particles have been studied intensively, questions about the detailed elementary steps of the ammonia formation reaction still remain.[10]

Gas-phase clusters can be used as a model to study such structure sensitive reactions; they are well-isolated and defined systems of limited and tractable size with a broad variety of different possible binding sites. This offers the chance to better understand the fundamental interplay between charge transfer and distribution, geometric and electronic structure, doping effects, etc., on the catalytic properties of metals.[11,12]

Despite this promising perspective, very little experimental information is available for free, i.e., not ligand-stabilized, ruthenium clusters. There is a report on measurements of the magnetic properties of neutral Ru clusters, concluding they have small magnetic moments,[13] and we have investigated CO binding to cationic and anionic Ru$_n^\pm$ clusters by infrared multiple photon dissociation (IR-MPD) spectroscopy on Ru$_n$CO$^\pm$ complexes. Molecularly adsorbed CO was found to bind predominantly at atop sites (μ_1), a few cluster sizes also showed signatures of bridge-bound (μ_2) CO molecules.[14] To our knowledge, no further experimental work on gas-phase ruthenium clusters has been published. The only other reports on mass selected ruthenium clusters are resonance enhanced Raman studies on the ruthenium dimer and trimer in cryogenic matrices.[15,16]

A number of theoretical studies have dealt with the description of ruthenium clusters (see refs 17−22 and references therein); however, problems arise from the presence of numerous low-lying excited states associated with the open 4d shells in Ru. In general, the favored structures are very sensitive to the level of theory. Even within density-functional theory (DFT), very different results can be obtained, depending on how the exchange correlation is treated. For example, functionals using the general-gradient approximation (GGA) favor unusual square or cubic structures for Ru.[20] Wang and Johnson argue that these structures are the result of using GGA functionals and show that hybrid functionals with partially exact exchange, like PBE0, lead to better agreement to high-level calculations and the experimental results available for Ru$_2$ and Ru$_3$.[21]

As mentioned above, the rate-determining step of ammonia synthesis on extended ruthenium surfaces is the dissociation of N$_2$.[7] To target the first step of this highly structure sensitive reaction, we aim to investigate activated N$_2$ molecules

chemisorbed on neutral Ru_n clusters ($n = 5-16$) by measuring their N−N stretching frequencies using IR-MPD spectroscopy.

II. EXPERIMENTAL METHODS

The IR-MPD spectra presented in this work have been measured with a pulsed molecular beam apparatus using the Free Electron Laser for Infrared eXperiments (FELIX) facility[23] in The Netherlands as the IR radiation source. Both the setup and the spectra recording technique have been described in detail elsewhere.[24]

As a summary, the experiment works as follows. A rotating and translating rod of ruthenium serves as the target in a laser ablation source. The resulting plasma is quenched by a pulse of He carrier gas, leading to cluster growth and thermalization to ∼30 °C. A pulse of N_2 is introduced further downstream in a reaction channel. After this channel the molecular beam expands into a vacuum, passing through a skimmer and an aperture that is held at a constant positive voltage to deflect all charged clusters from the beam. The remaining neutral clusters are then ionized using an F_2 laser (7.9 eV/photon) in the acceleration region of a reflectron time-of-flight mass spectrometer. The resulting mass spectra are recorded at 10 Hz. On every other shot the FELIX beam irradiates the cluster distribution. If an IR active internal vibration of the cluster complex is in resonance one or more IR photons can be absorbed and the resulting heating can lead to dissociation. The cluster size and coverage specific IR-MPD spectra can then be extracted by monitoring the changes induced in the mass distributions of the individual complexes as a function of the IR wavelength. To ensure that only irradiated clusters are analyzed, the FELIX beam counter propagates the molecular beam and is focused between skimmer and aperture.

III. RESULTS AND DISCUSSION

The product distribution of the reaction of thermalized neutral Ru clusters with molecular N_2 and subsequent ionization at 7.9 eV is shown in Figure 1. Ru_nN_{2m} species are found to dominate compared to odd-numbered nitrogen complexes. This implies that we mainly observe the addition of molecular nitrogen to the clusters and not addition of dissociated atomic N, produced in the ablation plasma. Further, it suggests that fragmentation processes involving loss of nitride species are minor channels.

The observed mass distribution will depend on the ionization energies (IEs) of the clusters. Unfortunately, there is hardly any experimental information for Ru clusters, and the IEs are not known. We can, however, make a comparison to the case of iron, which, in the bulk, has similar chemistry. There, the IEs have been measured[25,26] and drop with increasing size from the atomic value of 7.9 eV toward the bulk work function of ∼4.5 eV.[27] In the size range of $n = 6-16$, the IEs vary between 5.96 and 5.42 eV. Given that the IE of the ruthenium atom is 7.36 eV and the bulk work function 4.7 eV,[27] we can expect the IEs of the Ru clusters to be comparable, probably slightly lower, but we cannot rule out that certain sizes show particularly high or low values, which might influence their relative intensities in the mass spectrum. The influence of N_2 binding on the IEs of the investigated cluster complexes is not known. For physisorbed N_2, one would expect a lowered IE, but for chemisorbed N_2, the influence depends on the exact binding situation. However, given the expected IE values for the bare ruthenium clusters of about 5.5 eV, the change would need to be significant to influence the ionization efficiency at 7.9 eV. For comparison,
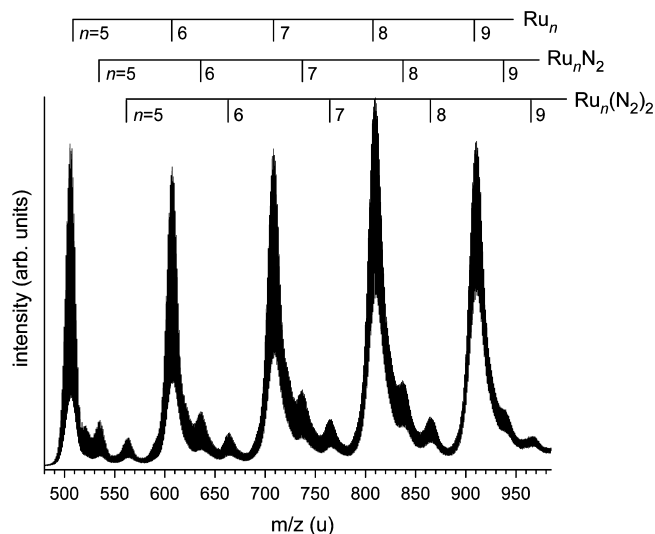

Figure 1. Part of the mass spectrum of Ru_nN_{2m} ($n = 5-9$; $m = 1, 2$) complexes ionized at 7.9 eV. The most intense peaks correspond to the bare ruthenium clusters, and the less intense peaks are the respective N_2 and $(N_2)_2$ complexes. For $n = 5$, a small signal between the bare cluster and the N_2 complex can be seen that may be attributed to a Ru_5N species. The single nitrogen atoms probably stem from N_2 molecules dissociated on the surface of the target or in the plasma. The resolution of the experiment ($m/\Delta m \approx 1200$) is sufficient to resolve the individual mass peaks in this cluster size range, which is not fully reproduced in the figure.

chemisorption of one or two O atoms on Nb clusters typically changes the IE by less than 0.3 eV.[28]

One general problem arising in studies of ruthenium clusters with mass spectrometric methods is the broad isotopic distribution of ruthenium (6% ^{96}Ru, 2% ^{98}Ru, 13% ^{99}Ru, 13% ^{100}Ru, 17% ^{101}Ru, 32% ^{102}Ru, 19% ^{104}Ru). Not only is the intensity of the Ru_n clusters distributed over many mass channels but the distributions for different species start to overlap with increasing cluster size. This overlap is particularly big for the very intense bare clusters and their respective N_2 complexes. Therefore, selectively studying the Ru_nN_2 complexes proved to be very difficult, and we have added slightly more N_2 to also form the $Ru_n(N_2)_2$ species.

The broad isotopic pattern also makes it difficult to determine if there are contaminants in the molecular beam, particularly with masses similar to N_2. To estimate the possible content of such contaminant species, we have fitted a simulation of the isotopic pattern of Ru_5 and Ru_6 and their respective complexes with N, N_2, and $(N_2)_2$ to the experimentally observed mass spectrum. The simulation correctly reproduces the bare metal peaks and the single nitrogen complexes, but the mass distributions corresponding to N_2 and $(N_2)_2$ complexes are slightly shifted to higher masses. Including a fraction of O_2 and N_2O_2 adducts in the simulation results in a better fit; the respective plots can be found in the Supporting Information. From the simulation we estimate the O_2 and N_2O_2 contamination to be on the order of 20%, which is surprisingly high. We assume that the respective O_2 is introduced with the N_2 gas. Given the high reactivity of oxygen toward ruthenium, even small contaminations could cause such an effect. This might influence our reactivity estimation (see below) if there are big differences in the reactivity of the ruthenium clusters toward oxygen in the investigated cluster

size range. It does not, however, influence the band positions measured by IR-MPD, as will be discussed below.

Despite the problems described above of possible contamination, we have tried to establish the relative reactivities of the Ru_n clusters toward nitrogen. The overlap between the intense bare metal peaks and their respective N_2 complexes complicates this estimation, but for the size range investigated, the $(N_2)_2$ complex is always well-separated and the N_2 complex is clearly identifiable as a shoulder on the mass distribution of the bare metal clusters. To determine the relative reactivities, the intensities of these features are analyzed by fitting Gaussian functions to the envelopes of the isotopic distributions. The increasing uncertainty due to the overlap is reflected in rather big error bars for the larger sizes, as can be seen in Figure 2. In
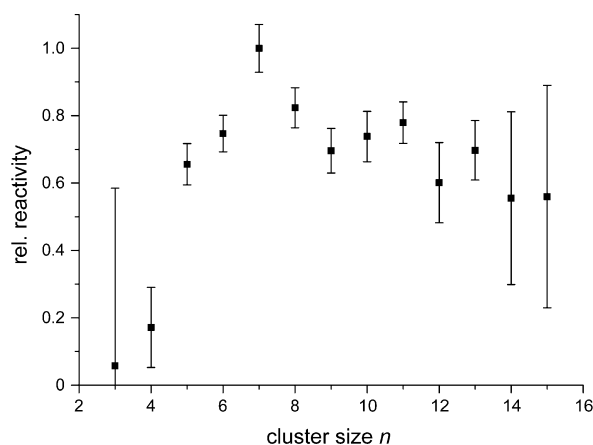

Figure 2. Reactivity of neutral Ru clusters with N_2 as a function of cluster size. The reactivity of Ru_n is defined as the ratio of the total abundance of the corresponding Ru_nN_{2m} ($m = 1, 2$) complexes and the sum of the abundances of bare Ru_n cluster and complexes. For this, the mass distribution shown in Figure 1 has been analyzed and the abundances are determined from fitting Gaussians to the envelopes of the isotopic distributions. Finally, the reactivity is normalized to that of the most reactive cluster size, i.e. Ru_7.

the size range investigated the reactivity varies only slightly (Figure 2), but a clear nonmonotonic behavior can be observed. This can be compared to the results of former reactivity studies of N_2 with tungsten and molybdenum clusters, which showed even more extreme variations of the reaction rate with cluster size, changing by several orders of magnitude.[29,30] Cluster sizes smaller than Ru_5 show low reactivity, and a weak maximum is reached at $n = 7$; the slightly lower reactivity of Ru_9 becomes also apparent in Figure 1.

To probe for the presence of molecularly bound N_2, we investigated the spectral range of 1300–2300 cm^{-1}, which covers the typical frequencies of the different N_2 species known to exist on transition metal surfaces. In addition to the physisorbed δ-state, there are at least two chemisorbed forms, the α-state and the γ-state,[31] that differ by their binding mechanisms. In the α-state π-bonded N_2 is oriented nearly parallel to the surface, while in the γ-state σ-bonded N_2 is oriented perpendicularly to the surface. To our knowledge, on Ru surfaces and in Ru complexes only δ- and γ-states have been observed (see below). In the physisorbed δ-state, there is almost no shift in the N–N stretching frequency[32] compared to the stretching frequency of unbound N_2 (2330 cm^{-1}), whereas the γ-state leads to significant red shifts of up to 140 cm^{-1}.[33] The α-state leads to even higher red shifts, for example, down

to 1555 cm^{-1} on Fe(111),[34] and despite its absence on Ru surfaces, it might be present on the clusters.

Figure 3 shows the depletion spectra for Ru_nN_2 (left) and $Ru_n(N_2)_2$ (right) ($n = 5-16$) in the range from 1900 to 2300

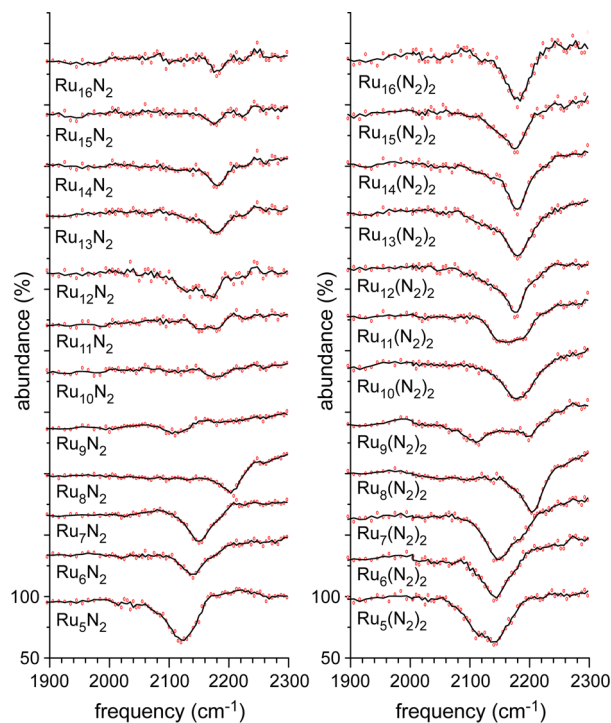**Figure 3.** IR-MPD spectra of neutral Ru_nN_2 (left) and $Ru_n(N_2)_2$ (right) complexes for $n = 5-16$. The open circles represent the measured data points; the lines are the respective binomially weighted five point averages.

cm^{-1}. Below 1900 cm^{-1} no bands are observed for any of the investigated complexes. The spectra of the $(N_2)_2$ complexes will be discussed first. Most complexes show a single band, located between 2100 and 2200 cm^{-1} and depleted by up to 40%. For $n = 9$, the situation is less clear; it appears that there are two relatively weak bands present, with about 15–25% depletion each, at 2110 and about 2195 cm^{-1}. This indicates the presence of (at least) two differently activated N_2 species for $Ru_9(N_2)_2$. It cannot be determined, however, if these exist within a single $Ru_9(N_2)_2$ complex or if there are several isomers present. The latter may explain the weaker apparent depletion per band compared to the other sizes showing only a single band. For most other sizes, the observed band shapes indicate a similar activation of all N_2 species contributing to the spectrum for a given composition, but it is still possible that isomers are present that contain slightly differently activated N_2 species which are not resolved in the spectra. $Ru_{11}(N_2)_2$ in particular has a relatively broad absorption band. However, Ru_9 is the only case where the bands are clearly separated.

The oxygen contaminants are not expected to have vibrational fundamentals in the range where we observe bands; therefore, they would not change our measured IR-MPD spectra, apart from leading to a smaller observed depletion, caused by the higher background of nondepletable species. A second possible influence is a shift in the N–N stretching frequency for $Ru_nN_2O_2$ species caused by the coadsorbed oxygen. However, the fraction of these species is small and a comparison of the Ru_nN_2 and $Ru_n(N_2)_2$ depletion

spectra does not suggest a significant influence (see below). A similar argument is also true for bare metal clusters overlapping with the N_2 mass distribution; they do not absorb in the investigated frequency range (typical metal–metal vibrations are below 450 cm^{-1})[35,36] but will only lead to a smaller apparent depletion.

The $\nu(N-N)$ band positions are determined by fitting with a Gaussian line shape to the depletion spectra, and their cluster size dependence is depicted in Figure 4, where for $n = 9$ the
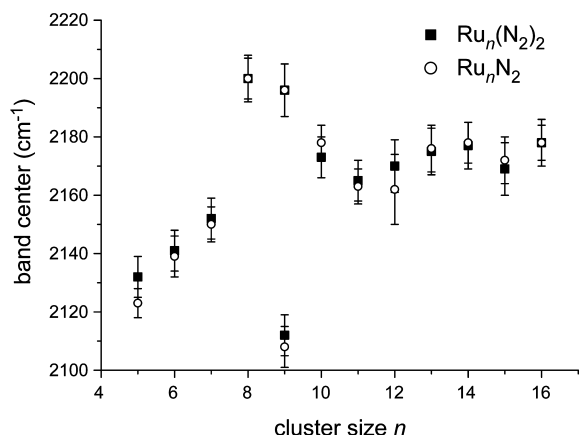

Figure 4. Band position of the $\nu(N-N)$ vibration for Ru_nN_2 (open circles) and $Ru_n(N_2)_2$ (black squares) complexes ($n = 5-16$). The error has two contributions: an uncertainty in the wavelength calibration of about 0.2% (~4 cm^{-1}) that applies equally to all values (thus not changing relative peak positions). The second contribution is an estimated part to account for deviations from a Gaussian line profile of the depletion bands.

existence of a second band is assumed; the respective Gaussian fits are shown in the Supporting Information. It should be noted, however, that above 2200 cm^{-1} the FELIX IR power drops significantly, possibly leading to a cutoff of the highest frequency bands observed, namely, the high frequency band of $Ru_9(N_2)_2$ and the band of $Ru_8(N_2)_2$.

All bands fall in the range between 2110 cm^{-1} for $n = 9$ and 2201 cm^{-1} for $n = 8$ and can be attributed to the N–N stretch of activated, γ-state bound N_2, supported by comparison with surface species and other N_2 containing species (see below), demonstrating the presence of cluster complexes with molecularly bound N_2. The apparent red shift from the vibration of free N_2 at 2330 cm^{-1} can be understood by a comparison with the isoelectronic CO. There, the binding mechanism is usually described with the Blyholder model[37] of σ-donation from the CO to the metal atom and π-back-donation from the metal d-orbitals into antibonding π^*-orbitals of the CO, thereby weakening the internal CO bond. This mechanism is similar to the one of γ-state bound N_2, and therefore, similar effects can be expected.

The $\nu(N-N)$ values rise smoothly for $n = 5-7$ from 2132 to 2152 cm^{-1}, followed by a strong increase of almost 50 cm^{-1} to 2201 cm^{-1} for $n = 8$. Assuming the presence of the second band for $n = 9$, this size then has two $\nu(N-N)$ frequencies at the extreme ends of measured values: 2110 cm^{-1} is by far the lowest value and 2195 cm^{-1} one of the highest. The latter value fits into the smooth decrease of $\nu(N-N)$ from $n = 8$ to 11, which is followed by a more or less constant value afterward up to $n = 16$.

Comparing Figures 2 and 4 reveals no clear correlation between the reactivity of the clusters and nitrogen activation in the complex, as one could intuitively expect. Ru_7 as the most reactive cluster shows one of the strongest N_2 activations in terms of $\nu(N-N)$, but for Ru_5 and Ru_6, which exhibit an even lower $\nu(N-N)$ in their complexes, a higher reactivity is not observed. Additionally, the least activating cluster, Ru_8, shows no particularly weak reactivity. Possibly the reaction kinetics are important for these clusters and we do not form an equilibrium distribution in our cluster source, but we can also not fully exclude the influence of very different IEs or reactivities toward O_2 that might partly explain the observed differences.

The presence of a significant fraction of $Ru_n(N_2)_2$ leads to some difficulties in the interpretation of the spectra for the Ru_nN_2 complexes, as fragmentation by N_2 loss into the lighter mass channel can disturb the measured depletion for the corresponding species. Nevertheless, for the smaller Ru_nN_2 ($n = 5-7$) complexes, clear bands are identified. A comparison with the depletion spectra of the $Ru_n(N_2)_2$ complexes reveals that the band positions for both types of complexes are very similar (see Figure 3), thus leading to a weaker apparent depletion in the spectra of the N_2 complexes. This contribution is significant, as the intensity of the $(N_2)_2$ complexes in the mass spectrum is about 40–60% of that of the N_2 complexes (depending on cluster size) and adds to the expected weaker depletion being caused by the increasing overlap between the bare metal peak and N_2 complexes that is increasing with cluster size. The decrease in signal caused by the depleting $Ru_n(N_2)_2$ complexes can be roughly corrected using the plausible assumptions that all (or at least the vast majority of the) dissociation in the $(N_2)_2$ complexes is caused by the loss of a single N_2 molecule and that there is no significant dissociation into the $(N_2)_2$ channel from $(N_2)_3$ complexes. Such corrected depletion spectra are provided in the Supporting Information, together with the Gaussian fits that have been used to determine the band positions of the N_2 absorption shown in Figure 4. In principle, the spectra of the $Ru_n(N_2)_2$ complexes may be similarly influenced by depletion of $Ru_n(N_2)_3$ complexes. However, the amount of the latter complexes is small compared to the N_2 and $(N_2)_2$ complexes, so that their influence can be neglected.

It should be noted explicitly that the method used here is only sensitive to molecularly bound N_2. Consequently, we are not able to detect Ru_nN_2 species with dissociated N_2, which might be present in the molecular beam. For $Ru_n(N_2)_2$ species, it is possible that the first N_2 molecule dissociates on the cluster and that we are probing the second, molecularly bound one, although this seems unlikely. If these species exist, the dissociated nitrogen atoms do not appear to change the activation of the N_2 molecule, as can be seen by the similar band positions of the Ru_nN_2 complexes and the respective $Ru_n(N_2)_2$ species.

A comparison of the N–N stretching frequencies found here with those of N_2 adsorbed on extended transition metal surfaces reveals that they are rather similar to those of the γ-state, representing chemisorbed, σ-bonded N_2 oriented perpendicularly to the surface. There is no indication of the presence of either the physisorbed δ-state or the more strongly activated π-bound α-state N_2, although they cannot be fully excluded. We would probably be blind to δ-state species as their absorption frequency will be close to the free gas-phase value of 2330 cm^{-1}, but they are unlikely to survive at the room temperature conditions of our experiment. The α-state could be

present in the beam, but we might be unable to deplete these species, possibly due to low IR cross sections and/or the need to absorb a larger number of photons to dissociate the complex as compared to the γ-state.

Unfortunately, further information about the binding geometry, i.e., if the N_2 molecule binds in atop, bridge, or hollow configuration, cannot be extracted from the stretching frequency alone, in contrast to the case of CO.[14] For Ru(001), the frequencies range from 2189 cm^{-1} for high coverages of N_2 to 2209 cm^{-1} for low coverages,[33] while for Ru(1010) a value of 2192 cm^{-1} has been reported.[38] For $n = 5-7$ and for the low frequency band in $n = 9$, the $\nu(N-N)$ values found in our experiment are considerably red-shifted compared to the reported surface values. This indicates a stronger activation of the N_2 molecule in these complexes and may be related to the presence of metal atoms of lower coordination compared to the regular surfaces. Similar values for $\nu(N-N)$ are also found in matrix isolation IR spectroscopy experiments on Ru(N$_2$)$_5$ species[39] ranging from 2147 to 2152.2 cm^{-1} and in dinitrogen complexes of atomic ruthenium, e.g., Ru(NH$_3$)$_5$N$_2$X$_2$ (X = Cl$^-$, Br$^-$, I$^-$) both in solid state and in various solutions, yielding values between 2085 and 2122 cm^{-1}.[40]

The large changes of the $\nu(N-N)$ frequency with cluster size are difficult to compare to similar changes of the CO stretching frequency on transition metal clusters. There, the CO molecules always bind via the C atom and the CO is perpendicular to the cluster surface, as in the case of the γ-state for N_2. The different binding geometries (atop, bridge, hollow) can, however, be distinguished on the basis of the frequency of the $\nu(C-O)$ stretch, as they differ in frequency by more than 150 cm^{-1}.[14] Such a clear distinction is not reported for N_2. Consequently, we are unable to determine if the shifts observed in $\nu(N-N)$, especially for $n = 8$ and 9, are due to different binding geometries or due to other factors, for example, differences in the electronic or geometric structures of the ruthenium clusters. Nevertheless, a comparison of the variation of the observed $\nu(N-N)$ frequencies with cluster size with those of $\nu(C-O)$ might still be interesting to detect possible similar trends. For cationic Ru$_n$CO$^+$, nonmonotonic behavior of $\nu(C-O)$ was also found for $n = 8$ and 9, showing an exceptionally high frequency for the former and an exceptionally low one for the latter, though both probably contain atop-bound CO.[14] The similarity to our observations suggests that the same geometric or electronic effect may be responsible for the lower activation induced by Ru$_8$ and the higher one by Ru$_9$, respectively.

To determine whether it is geometric or electronic factors which are responsible for the large differences in the N_2 activation observed, structural information for the Ru clusters would be necessary. Several purely theoretical studies have dealt with these clusters, and some of them have predicted structures in the size range we have investigated.[17,18] It has, however, been shown for small Ru clusters that the results of DFT calculations are very sensitive to the choice of the exchange correlation functional and that hybrid functionals give different answers compared to nonhybrid ones,[21] similar to the case of rhodium clusters.[36] In contrast to rhodium clusters, unfortunately, there are no published experimental data to test the validity of these predictions. Therefore, we have to consider the structures of ruthenium clusters to still be undetermined, and the underlying causes of the large frequency shifts in both the neutral Ru$_n$N$_2$ and the cationic Ru$_n$CO$^+$ complexes remain, for the moment, unclear.

IV. CONCLUSION

The adsorption of one and two nitrogen molecules on neutral Ru clusters in the size range of 5−16 atoms has been investigated with IR-MPD spectroscopy. For all cluster sizes we identify molecular binding to be a major channel for both the first and the second N_2 molecule. The observed $\nu(N-N)$ frequencies suggest the presence of σ-bonded N_2 oriented perpendicularly to the surface, i.e., the γ-state for the N_2 binding on extended ruthenium surfaces. Both Ru$_8$N$_{2m}$ and Ru$_9$N$_{2m}$ show interesting differences compared to the other cluster size. For Ru$_9$N$_{2m}$ two $\nu(N-N)$ bands are observed, indicating the presence of two differently activated dinitrogen species. One of these bands is the lowest $\nu(N-N)$ frequency observed in this study, while the maximum is observed for Ru$_8$N$_{2m}$. Similar behavior is observed for CO bound to cationic ruthenium clusters, and these size-dependent differences in the activation of N_2 and CO might serve as a good benchmark for future calculations on these systems.

■ ASSOCIATED CONTENT

S Supporting Information

Comparison of simulated isotopic patterns for complexes of Ru$_5$ and Ru$_6$ with the experimental mass spectrum, IR-MPD spectra of neutral Ru$_n$(N$_2$)$_2$ complexes for $n = 5-16$ together with the Gaussian fits to determine the central band position, and reconstructed depletion spectra of the Ru$_n$N$_2$ complexes. This material is available free of charge via the Internet at http://pubs.acs.org

■ AUTHOR INFORMATION

Corresponding Author
*E-mail: fielicke@physik.tu-berlin.de.
Notes
The authors declare no competing financial interest.

■ ACKNOWLEDGMENTS

■ REFERENCES

(1) Blume, R.; Havecker, M.; Zafeiratos, S.; Teschner, D.; Kleimenov, E.; Knop-Gericke, A.; Schlogl, R.; Barinov, A.; Dudin, P.; Kiskinova, M. Catalytically Active States of Ru(0001) Catalyst in CO Oxidation Reaction. *J. Catal.* **2006**, *239*, 354−361.

(2) Jacobsen, C. J. H.; Dahl, S.; Hansen, P. L.; Tornqvist, E.; Jensen, L.; Topsoe, H.; Prip, D. V.; Moenshaug, P. B.; Chorkendorff, I. Structure Sensitivity of Supported Ruthenium Catalysts for Ammonia Synthesis. *J. Mol. Catal. A* **2000**, *163*, 19−26.

(3) Logadottir, A.; Rod, T. H.; Norskov, J. K.; Hammer, B.; Dahl, S.; Jacobsen, C. J. H. The Bronsted−Evans−Polanyi Relation and the Volcano Plot for Ammonia Synthesis over Transition Metal Catalysts. *J. Catal.* **2001**, *197*, 229−231.

(4) Aika, K. I.; Ozaki, A. Kinetics and Isotope Effect of Ammonia Synthesis over Ruthenium. *J. Catal.* **1970**, *16*, 97−101.

(5) Aika, K.; Ozaki, A.; Hori, H. Activation of Nitrogen by Alkali-Metal Promoted Transition-Metal 1. Ammonia Synthesis over Ruthenium Promoted by Alkali-Metal. *J. Catal.* **1972**, *27*, 424−431.

(6) Bielawa, H.; Hinrichsen, O.; Birkner, A.; Muhler, M. The Ammonia-Synthesis Catalyst of the Next Generation: Barium-Promoted Oxide-Supported Ruthenium. *Angew. Chem., Int. Ed.* **2001**, *40*, 1061−1063.

(7) Logadottir, A.; Norskov, J. K. Ammonia Synthesis over a Ru(0001) Surface Studied by Density Functional Calculations. *J. Catal.* **2003**, *220*, 273−279.

(8) Shetty, S.; Jansen, A. P. J.; van Santen, R. A. Active Sites for N_2 Dissociation on Ruthenium. *J. Phys. Chem. C* **2008**, *112*, 17768−17771.

(9) Hansen, T. W.; Hansen, P. L.; Dahl, S.; Jacobsen, C. J. H. Support Effect and Active Sites on Promoted Ruthenium Catalysts for Ammonia Synthesis. *Catal. Lett.* **2002**, *84*, 7−12.

(10) Schlögl, R. Catalytic Synthesis of Ammonia—A "Never-Ending Story"? *Angew. Chem., Int. Ed.* **2003**, *42*, 2004−2008.

(11) Knickelbein, M. B. Reactions of Transition Metal Clusters with Small Molecules. *Annu. Rev. Phys. Chem.* **1999**, *50*, 79−115.

(12) Lang, S. M.; Bernhardt, T. M. Gas Phase Metal Cluster Model Systems for Heterogeneous Catalysis. *Phys. Chem. Chem. Phys.* **2012**, *14*, 9255−9269.

(13) Cox, A. J.; Louderback, J. G.; Apsel, S. E.; Bloomfield, L. A. Magnetism in 4d-Transition Metal-Clusters. *Phys. Rev. B* **1994**, *49*, 12295−12298.

(14) Lyon, J. T.; Gruene, P.; Fielicke, A.; Meijer, G.; Rayner, D. M. Probing C-O Bond Activation on Gas-Phase Transition Metal Clusters: Infrared Multiple Photon Dissociation Spectroscopy of Fe, Ru, Re, and W Cluster CO Complexes. *J. Chem. Phys.* **2009**, *131*.

(15) Wang, H. M.; Liu, Y. F.; Haouari, H.; Craig, R.; Lombardi, J. R.; Lindsay, D. M. Raman Spectra of Ruthenium Dimers. *J. Chem. Phys.* **1997**, *106*, 6534−6537.

(16) Fang, L.; Shen, X. L.; Chen, X. Y.; Lombardi, J. R. Raman Spectra of Ruthenium and Tantalum Trimers in Argon Matrices. *Chem. Phys. Lett.* **2000**, *332*, 299−302.

(17) Zhang, W. Q.; Zhao, H. T.; Wang, L. C. The Simple Cubic Structure of Ruthenium Clusters. *J. Phys. Chem. B* **2004**, *108*, 2140−2147.

(18) Li, S. F.; Li, H. S.; Liu, J.; Xue, X. L.; Tian, Y. T.; He, H.; Jia, Y. Structural and Electronic Properties of Ru_n Clusters (n = 2−14) Studied by First-Principles Calculations. *Phys. Rev. B* **2007**, *76*, 045410.

(19) Rösch, N.; Petrova, G.; Petkov, P.; Genest, A.; Krüger, S.; Aleksandrov, H.; Vayssilov, G. Impurity Atoms on Small Transition Metal Clusters. Insights from Density Functional Model Studies. *Top. Catal.* **2011**, *54*, 363−377.

(20) Shunfang, L.; Haisheng, L.; Jing, L.; Xinlian, X.; Yongtao, T.; Hao, H.; Yu, J. Structural and Electronic Properties of Ru_n Clusters (n=2−14) Studied by First-Principles Calculations. *Phys. Rev., B, Condens, Matter Mater. Phys.* **2007**, *76*, 1−99.

(21) Wang, L. L.; Johnson, D. D. Removing Critical Errors for DFT Applications to Transition-Metal Nanoclusters: Correct Ground-State Structures of Ru Clusters. *J. Phys. Chem. B* **2005**, *109*, 23113−23117.

(22) Shetty, S.; Jansen, A. P. J.; van Santen, R. A. Magnetic, Bonding and Structural Behavior of Ru_{12} and Ru_{13} Clusters: Is Ru_{12} Magic? *THEOCHEM J. Mol. Struct.* **2010**, *954*, 109−114.

(23) Oepts, D.; van der Meer, A. F. G.; van Amersfoort, P. W. The Free-Electron-Laser User Facility Felix. *Infrared Phys. Technol.* **1995**, *36*, 297−308.

(24) Fielicke, A.; von Helden, G.; Meijer, G.; Pedersen, D. B.; Simard, B.; Rayner, D. M. Size and Charge Effects on the Binding of CO to Small Isolated Rhodium Clusters. *J. Phys. Chem. B* **2004**, *108*, 14591−14598.

(25) Yang, S.; Knickelbein, M. B. Photoionization Studies of Transition-Metal Clusters—Ionization-Potentials for Fe_n and Co_n. *J. Chem. Phys.* **1990**, *93*, 1533−1539.

(26) Rohlfing, E. A.; Cox, D. M.; Kaldor, A. Photoionization Measurements on Isolated Iron-Atom Clusters. *Chem. Phys. Lett.* **1983**, *99*, 161−166.

(27) *CRC Handbook of Chemistry and Physics*, 82 ed.; Lide, D. R., Ed.; CRC Press: Boca Raton, FL, 2001.

(28) Athanassenas, K.; Kreisle, D.; Collings, B. A.; Rayner, D. M.; Hackett, P. A. Ionization Potentials of Niobium Cluster Oxides. *Chem. Phys. Lett.* **1993**, *213*, 105−110.

(29) Mitchell, S. A.; Lian, L.; Rayner, D. M.; Hackett, P. A. Reaction of Molybdenum Clusters with Molecular Nitrogen. *J. Chem. Phys.* **1995**, *103*, 5539−5547.

(30) Mitchell, S. A.; Rayner, D. M.; Bartlett, T.; Hackett, P. A. Reaction of Tungsten Clusters with Molecular Nitrogen. *J. Chem. Phys.* **1996**, *104*, 4012−4018.

(31) Grunze, M.; Strasser, G.; Golze, M.; Hirschwald, W. Thermodynamic and Kinetic-Parameters of Molecular Nitrogen Adsorption on Fe(111). *J. Vac. Sci. Technol. A-Vac. Surf. Films* **1987**, *5*, 527−534.

(32) Shi, H.; Jacobi, K. Evidence for Physisorbed N_2 in the Monolayer on Ru(001) at 40 K. *Surf. Sci.* **1992**, *278*, 281−285.

(33) Depaola, R. A.; Hoffmann, F. M.; Heskett, D.; Plummer, E. W. Absorption of Molecular Nitrogen on Clean and Modified Ru(001) Surfaces—The Role of Sigma-Bonding. *Phys. Rev. B* **1987**, *35*, 4236−4249.

(34) Tsai, M. C.; Seip, U.; Bassignana, I. C.; Kuppers, J.; Ertl, G. A Vibrational Spectroscopy Study on the Interaction of N_2 with Clean and K-Promoted Fe(111) Surfaces—Pi-Bonded Dinitrogen as Precursor for Dissociation. *Surf. Sci.* **1985**, *155*, 387−399.

(35) Fielicke, A.; Kirilyuk, A.; Ratsch, C.; Behler, J.; Scheffler, M.; von Helden, G.; Meijer, G. Structure Determination of Isolated Metal Clusters Via Far-Infrared Spectroscopy. *Phys. Rev. Lett.* **2004**, *93*, 023401.

(36) Harding, D. J.; Walsh, T. R.; Hamilton, S. M.; Hopkins, W. S.; Mackenzie, S. R.; Gruene, P.; Haertelt, M.; Meijer, G.; Fielicke, A. Communications: The Structure of Rh_8^+ in the Gas Phase. *J. Chem. Phys.* **2010**, *132*, 011101.

(37) Blyholder, G. Molecular Orbital View of Chemisorbed Carbon Monoxide. *J. Phys. Chem.* **1964**, *68*, 2772−2777.

(38) Gruyters, M.; Jacobi, K. High-Resolution Electron-Energy-Loss Spectroscopy Study of Chemisorbed and Physisorbed N_2 on Ru(1010). *Surf. Sci.* **1995**, *336*, 314−320.

(39) Citra, A.; Andrews, L. Reactions of Laser-Ablated Osmium and Ruthenium Atoms with Nitrogen. Matrix Infrared Spectra and Density Functional Calculations of Osmium and Ruthenium Nitrides and Dinitrides. *J. Phys. Chem. A* **2000**, *104*, 1152−1161.

(40) Folkesson, B. Infrared-Absorption Intensities of N−N and M−N_2 Stretching Vibrations in Ruthenium and Osmium Dinitrogen Complexes. *Acta Chem. Scand.* **1972**, *26*, 4008−4018.

12158

dx.doi.org/10.1021/jp401876b | *J. Phys. Chem. C* 2013, 117, 12153−12158